

Protein aggregation in salt solutions

Miha Kastelic^a, Yuriy V. Kalyuzhnyi^b, Barbara Hribar-Lee^a, Ken A. Dill^{c,1}, and
Vojko Vlachy^a

^aFaculty of Chemistry and Chemical Technology, University of Ljubljana, 1000 Ljubljana, Slovenia;

^bInstitute for Condensed Matter Physics, 79011 Lviv, Ukraine;

and ^cLaufer Center for Physical and Quantitative Biology and Departments of Physics and Chemistry, Stony Brook University, Stony Brook, NY 11794.

Contributed by Ken A. Dill, April 20, 2015 (sent for review January 16, 2015; reviewed by Shekhar Garde and John M. Prausnitz)

报告人：王帅
信息学院

the process of protein aggregation
is important in many ways

- first: a key step in developing biotech drugs
- second: protein aggregation in the cell plays a key role in protein condensation diseases
- third: protein crystals, a particular state of protein aggregation

Main content

- We **model a protein** as having multiple binding sites to other proteins, leading to orientational variations, dependent on salt. With few parameters and with knowledge of the cloud-point temperatures as a function of added salt, **the model gives good predictions for properties including** the liquid–liquid coexistence curves, the second virial coefficients, and others for lysozyme and gamma-crystallin.

protein aggregation is poorly understood

1. **Atomistic-level molecular simulations** are not practical for studying multiprotein interactions as a function of concentration, **In liquid solutions** that are themselves fairly complicated.
2. Adapt colloid theories—DLVO theory.
3. However, DLVO does not readily account for protein sequence-structure properties, salt bridges, explicit waters in general, or Hofmeister effects.
4. Coarse-grained statistical mechanics is essential for describing the properties of complex solutions.
5. Patchy models
6. A key conclusion from these works is that to **properly capture protein liquid-phase equilibria** seems to require that the range of interactions between proteins be short.

- Modeling proteins as rigid bodies has severe limitations.
- When analyzing protein aggregation by such models, these studies (Sarangapani et al, Prausnitz) indicate the importance of knowing that during the experiment the native structure is preserved.
- The cloud-point temperature measurements model.

浊点温度

- 浊点(CP) 是非离子表面活性剂(NS) 均匀胶束溶液发生相分离的温度，是其非常重要的物理参数。非离子表面活性剂由完全溶解转变为部分溶解，其转变时的温度即为浊点温度。

model proteins

- treat the protein–protein interaction as directional
- model proteins as hard spheres, with a number of square-well attractive sites called “binding sites” located on the surface
- treat the solution physics through the thermodynamic perturbation theory that was developed by Wertheim for liquids that are strongly associating.

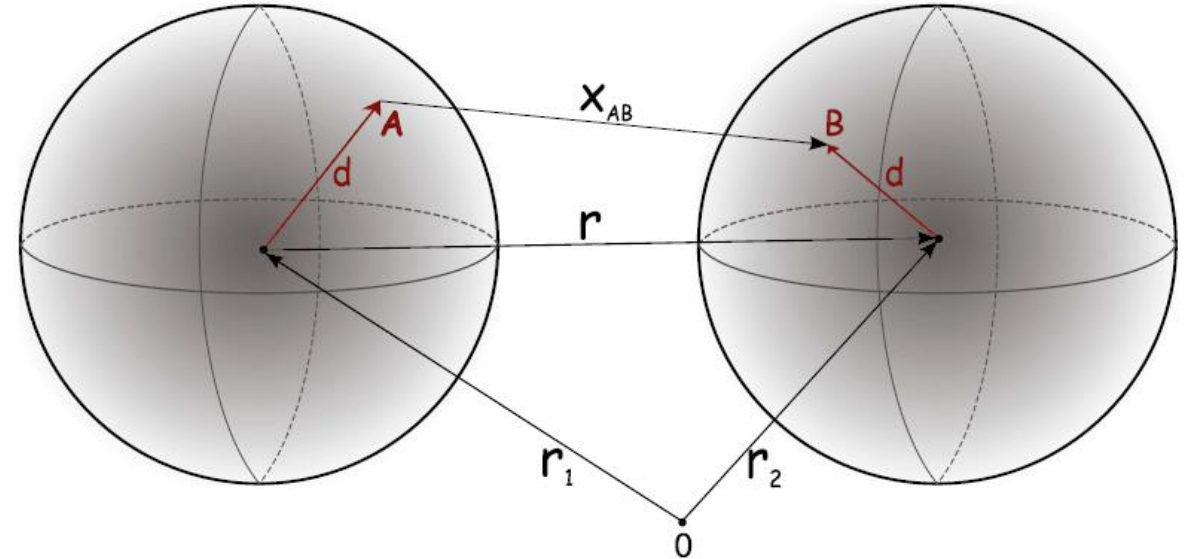


Fig. 1. Proteins interact as two spheres. They interact at $M \times M$ pairs of binding sites on the surfaces, one pair of which (A and B) is indicated here.

The methods of modeling the protein solution

- a one-component system of N protein molecules with number density $\rho=N/V$ at temperature T and volume V .
- The protein molecules are represented as spheres of diameter σ embedded in the solvent composed of water, buffer, and various simple salts.

The methods of modeling the protein solution

$$u(\mathbf{r}) = u_R(r) + \sum_{A \in \Gamma} \sum_{B \in \Gamma} u_{AB}(\mathbf{x}_{AB}).$$

$$u_R(r) = \begin{cases} \infty & \text{for } r < \sigma, \\ 0 & \text{for } r \geq \sigma, \end{cases}$$

$$u_{AB}(\mathbf{x}_{AB}) = \begin{cases} -\varepsilon W & \text{for } |\mathbf{x}_{AB}| < a_W, \\ 0 & \text{for } |\mathbf{x}_{AB}| \geq a_W. \end{cases}$$

$$0 < a_W < \sigma - \sqrt{3}d$$

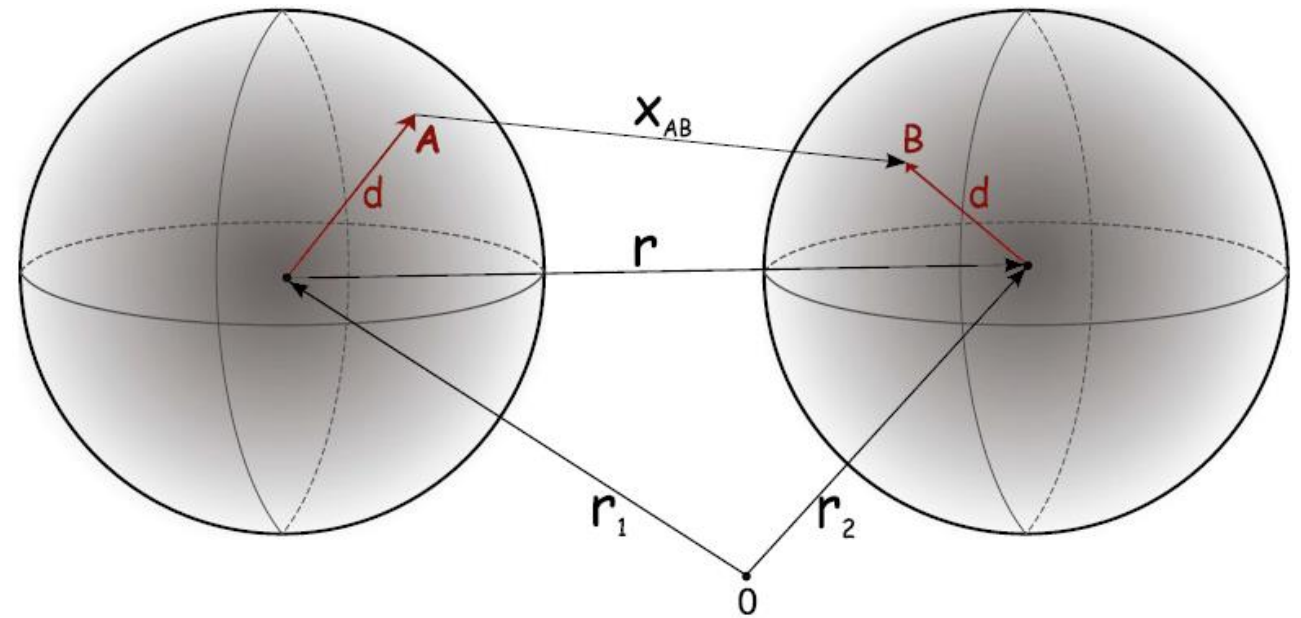


Fig. 1. Proteins interact as two spheres. They interact at $M \times M$ pairs of binding sites on the surfaces, one pair of which (A and B) is indicated here.

the calculation of the coexistence curve

$$A = A^{\text{id}} + A^{\text{hs}} + A^{\text{ass}}$$
$$\frac{\beta A^{\text{ass}}}{N} = M \left(\ln X - \frac{X}{2} + \frac{1}{2} \right)$$
$$X = \frac{1}{1 + MX\rho\Delta_{\text{AB}}}$$

$$\Delta_{\text{AB}} = 4\pi g^{\text{hs}}(\sigma) \int_{\sigma}^{2d+a_w} \bar{f}_{\text{ass}}(r) r^2 dr,$$

$$\mu = \left[\frac{\partial(A/V)}{\partial \rho} \right]_{T,V}$$

$$P = \rho\mu - \frac{A}{V}$$

$$\beta P = \rho + B_2\rho^2 + \dots$$

Numerical Results and Comparison with Experimental Data

- 1.obtain parameters of the model:
- M :the number of attractive square-well sites;mainly influence the critical density of the coexistence curve
- ϵ_W :influence the shape of coexistence curves;affects the critical temperature
- a_W :influence the shape of coexistence curves;determines the breadth of the coexistence curve.

- 2. $0 < a_W < \sigma - \sqrt{3}d$ fix $a_W = 0.18$ nm equal to the length of a hydrogen bond
- 3. set ϵ_W to get the correct critical temperature.
- We find best fits of $eW = 19.6$ kJ/mol for lysozyme and 20.7 kJ/mol for γ IIIa-crystallin.

Table 1. Model parameters used in the lysozyme and γ IIIa-crystallin calculations

Parameter	Lysozyme	γ IIIa-crystallin
σ , nm	3.43	3.78
M_2 , g·mol ⁻¹	14,300	20,700
M	10	14
ϵ_W/k_B , K	2,360	2,490
a_W , nm	0.18	0.18

Liquid–Liquid Coexistence Curves and Cloud-Point Temperatures

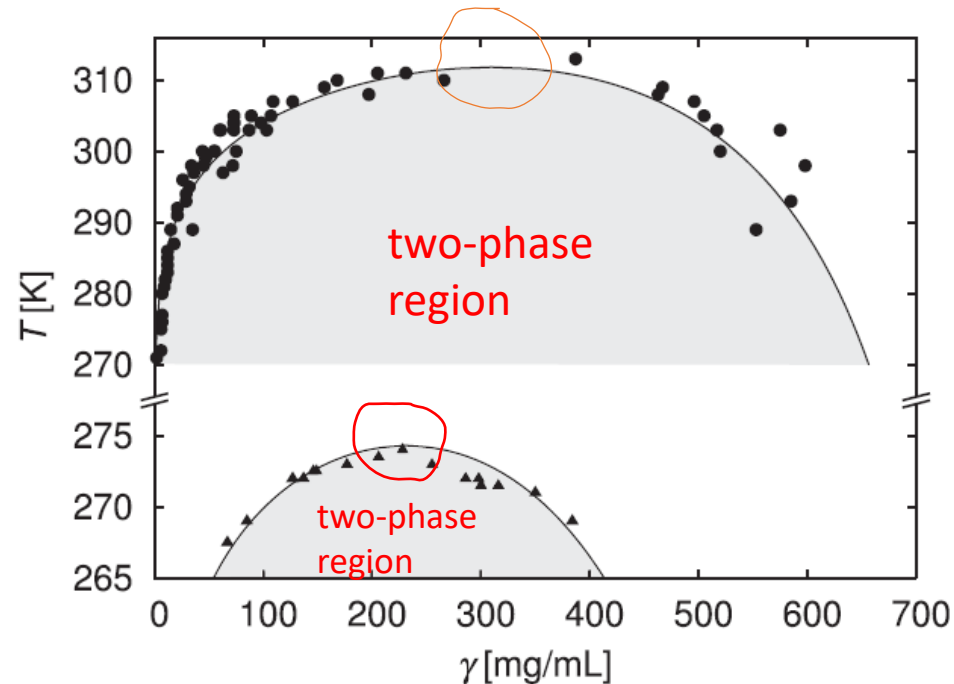


Fig. 2. Liquid–liquid phase separation, two-phase region is indicated by shaded area: lysozyme (\blacktriangle) (pH 6.0, phosphate buffer of ionic strength $0.6 \text{ mol}\cdot\text{dm}^{-3}$) (25) and γ IIIa-crystallin (\bullet) (pH 7.1, phosphate buffer, $0.24 \text{ mol}\cdot\text{dm}^{-3}$) (26) solutions. Solid curves are calculated from our model, based on the parameters in Table 1. The critical temperatures above which we have one-phase regions are estimated to be $274 \pm 2 \text{ K}$ for lysozyme and $312 \pm 2 \text{ K}$ for γ IIIa-crystallin.

- we fit our calculations to the experimental liquid–liquid phase diagrams of lysozyme and γ IIIa-crystallin published in refs. 25 and 26.

$$I_{\text{ion}} = 0$$

$$\gamma = \rho M_2 / N_A$$

Table 1. Model parameters used in the lysozyme and γ IIIa-crystallin calculations

Parameter	Lysozyme	γ IIIa-crystallin
σ , nm	3.43	3.78
M_2 , $\text{g}\cdot\text{mol}^{-1}$	14,300	20,700
M	10	14
ϵ_W/k_B , K	2,360	2,490
a_W , nm	0.18	0.18

M_2 is the molar mass of the protein.

Study protein' T_{cloud} associated with **salt effect**

- 前人的研究：Taratuta et al. determined cloud-point temperatures for lysozyme–phosphate buffer mixtures. At buffer ionic strengths ranging from 0.3 to 0.6 mol·dm⁻³ (at pH 6.8), found no change in the cloud-point temperature.

原因 This can be attributed to the **strong electrostatic screening** of the protein–protein charge interactions at high buffer concentration.

Study protein' T_{cloud} associated with salt effect

- Taratuta et al. also studied the effects of **added alkali-halide salts** (NaCl, KCl, NaBr, and KBr) to the solution, at the same time decreasing the buffer content to keep the total ionic strength, I_{tot} , fixed at $0.6 \text{ mol}\cdot\text{dm}^{-3}$

原因 increased attraction between protein molecules at increased alkali-halide salt ionic strength I_{ion}

experimental data (pH, I_{tot} , phosphate buffer and added alkali-halide salts)

原因 specific-salt effects occurring at the protein surface

$$\epsilon_{\text{W}}(I_{\text{ion}})/k_{\text{B}} = a \cdot I_{\text{ion}} + b \quad \text{results of Eq. 12}$$

Table 2. Parameters a ($\text{K}\cdot\text{dm}^3\cdot\text{mol}^{-1}$) and $b = 2,374$ (K) defining Eq. 12

Parameter	KBr	KCl	NaBr	NaCl
a	1,000	290	790	238

2018/1/12

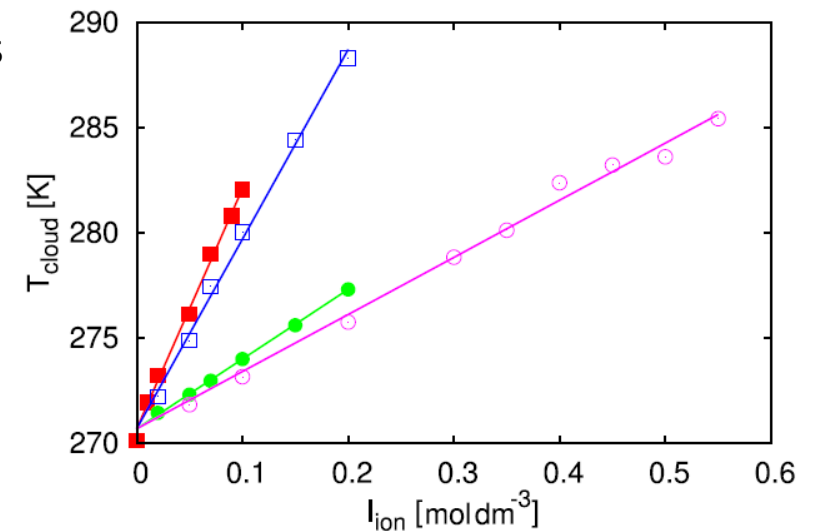


Fig. 3. T_{cloud} for lysozyme as a function of ionic strength of the added alkali-halide salts I_{ion} : symbols denote experimental data (pH 6.8, $I_{\text{tot}} = 0.6 \text{ mol}\cdot\text{dm}^{-3}$, phosphate buffer and added alkali-halide salts) (25) and the lines are results of Eq. 12. The parameters are from Table 2. From top to bottom: KBr (filled red square), NaBr (open blue square), KCl (filled green circle), and NaCl (open pink circle) salts.

model

$$\epsilon_W(I_{\text{ion}})/k_B = a \cdot I_{\text{ion}} + b$$

Table 2. Parameters a ($\text{K}\cdot\text{dm}^3\cdot\text{mol}^{-1}$) and $b = 2,374$ (K) defining Eq. 12

Parameter	KBr	KCl	NaBr	NaCl
a	1,000	290	790	238

当为 I_{ion} 零时(no alkali-halide salts present), 与Fig. 2类似。

In our simple model, the linearity between T_{cloud} and I_{ion} translates into the linear dependence of e_W on I_{ion} .

Prediction of model: One practical application of model

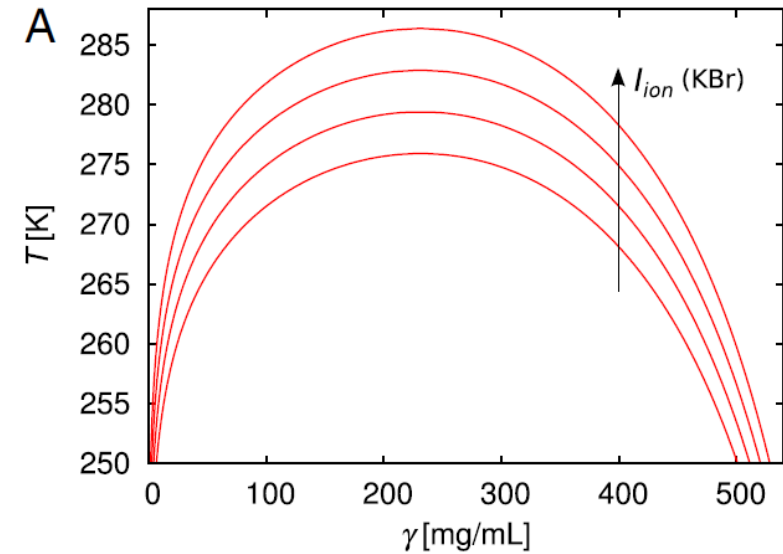


Fig. 4. The calculated coexistence curves for lysozyme in the buffer-salt mixtures. Calculations are based on Eq. 12 and parameters from Table 2. (A) KBr and (B) NaCl are added to the buffer keeping the total ionic strength $I_{tot} = 0.6 \text{ mol}\cdot\text{dm}^{-3}$ constant. Increase of I_{ion} (bottom to top) from 0 to $0.09 \text{ mol}\cdot\text{dm}^{-3}$ in steps of $0.03 \text{ mol}\cdot\text{dm}^{-3}$ (pH 6.8) causes an increase in the critical temperature.

$$I_{ion} \in [0, 0.09]$$

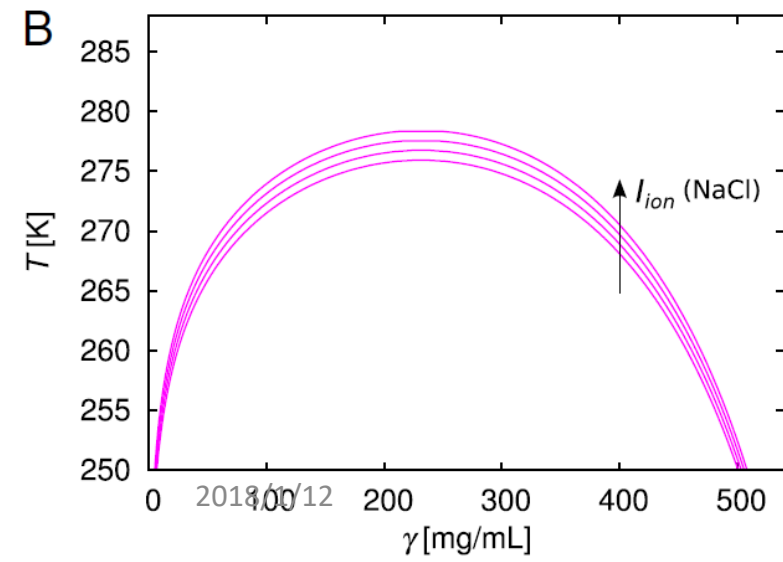


figure show: the critical temperature for protein aggregation is increased much more by adding KBr than by adding NaCl salt.
however: No experiments are yet available to test these full phase-diagram predictions

rationalize salt effects

- First: why should **the well depth** increase with ionic strength of added alkali-halide salts?
- 原因 The effect seems to be due to the adsorption of (halide)ions to the protein–solution surface
- 前人研究 Zhang and Cremer (40) showed that specific-salt dependence of T_{cloud} can be modeled by **a modified Langmuir binding isotherm.**

rationalize salt effects

- Second: can we rationalize the different effects of **different types of salts?**

It shows: ions that are most strongly solvated by water (which are the ions having the smallest radii, for atomic ions) are those that have the smallest effect (the smallest slopes a) on cloud-point temperatures.

The ions that most readily release hydration waters most strongly affect the protein–protein attraction.

The ordering of salts follows the so-called **inverse Hofmeister series**

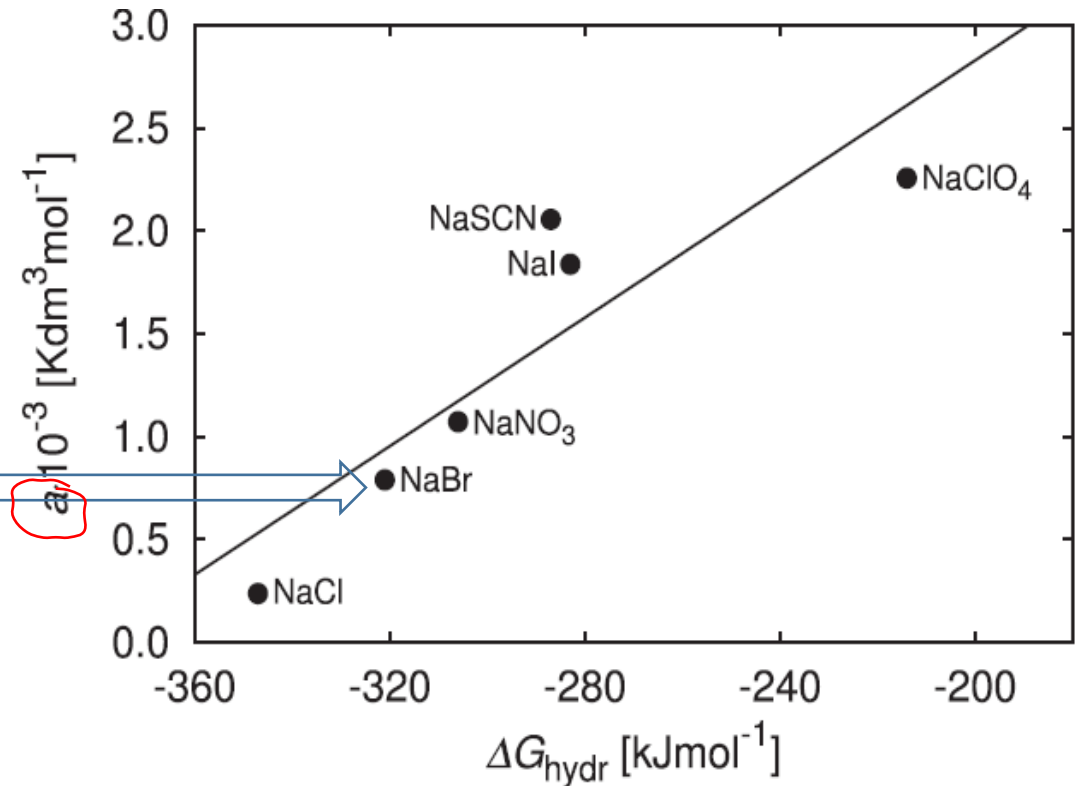


Fig. 5. Specific ion effects in lysozyme solutions: correlation of the slope a of Eq. 12 with the hydration Gibbs free energies ΔG_{hydr} (43) of the corresponding anions. The line is the **best least-square fit** through the data.

Second Virial Coefficient and Osmotic Compressibility

- **The second virial coefficient** is a principal measure of pairwise protein–protein interactions in solution
- In recent years, the second virial coefficient has become an important tool for understanding and **predicting protein crystallization conditions**
- George and Wilson were the first to notice that the conditions that **best promote protein crystallization** are those that fall within a particular “crystallization slot” of values of the second virial coefficient, B_{22} .
- **The favorable range of B_{22}** values for which proteins should crystallize from a water–salt mixture is between -2×10^{-4} and $-8 \times 10^{-4} \text{ cm}^3 \cdot \text{mol} \cdot \text{g}^{-2}$ (44, 49). **B_{22} is calculated on the basis** of the protein mass concentration γ and is related to B_2 in Eq. 11 as $B_{22} = B_2 N_A / M^2$.

- **Rarely** a given type of protein
- all of the properties of aggregation together
 - 1. T_{cloud}
 - 2. liquid–liquid phase coexistence curves
 - 3. B22
 - 4. χ_{osm}



Systematic
experiments

a virtue of the present model: From a single type of experiment, such as cloud-point measurements, we can compute all of the rest.

for example, Fig. 6 shows our calculated B_2 curves for lysozyme in buffer–salt mixtures under experimental conditions of Fig. 3.

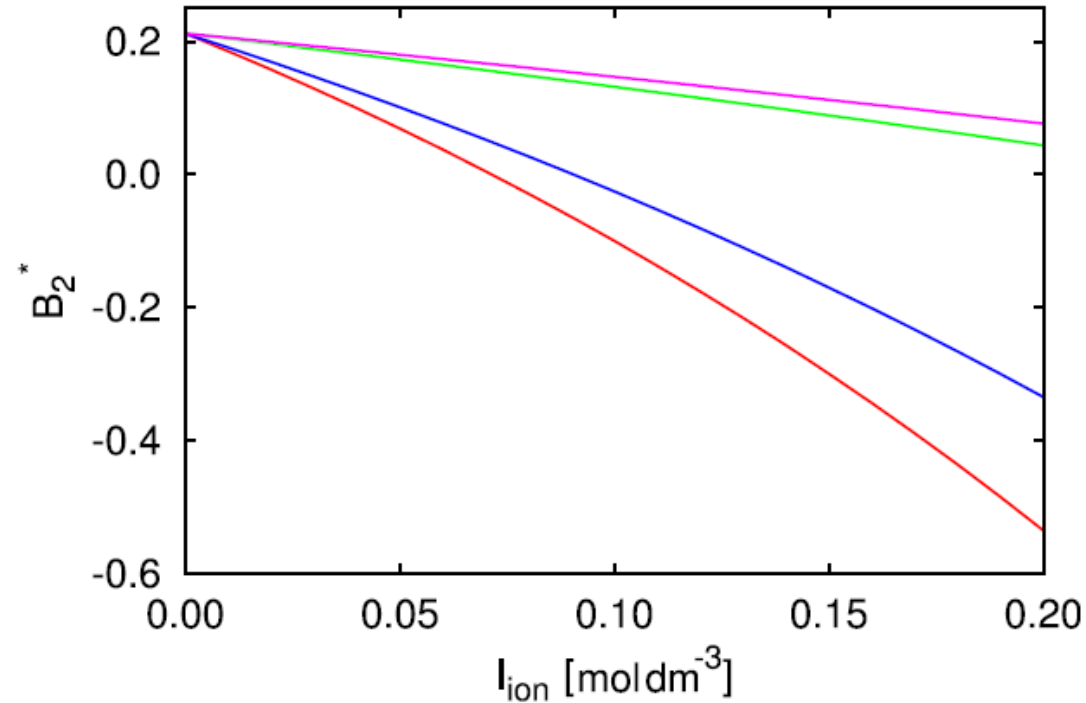
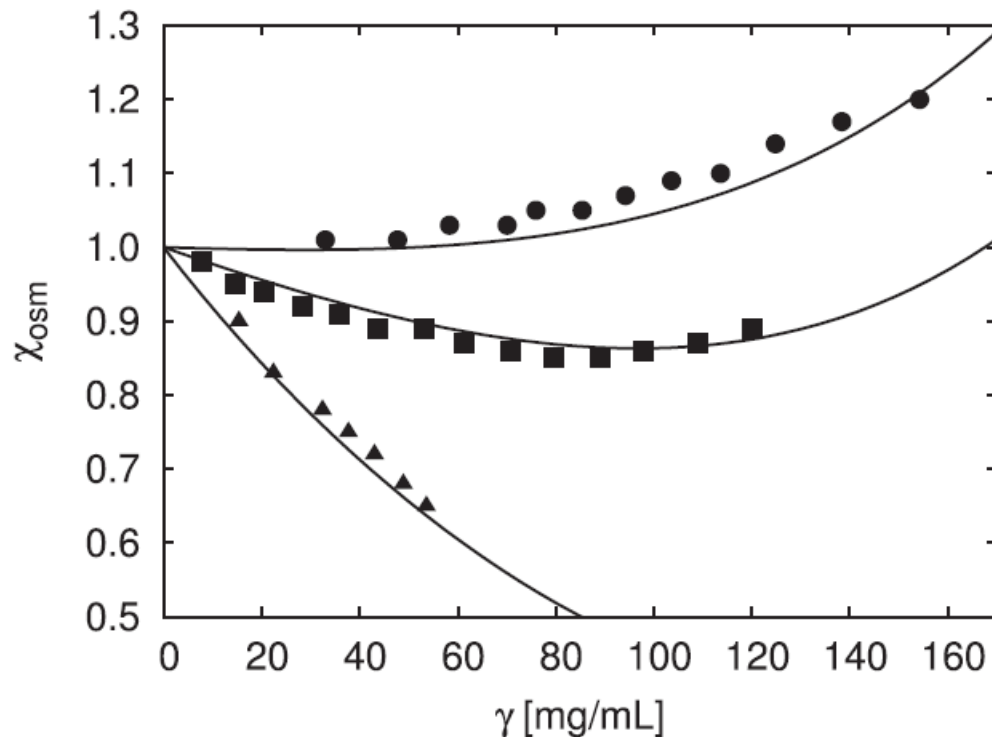


Fig. 6. Calculated B_2^* for lysozyme buffer – salt mixtures at $T = 300$ K: experimental conditions (pH 6.8, $I_{\text{tot}} = 0.6 \text{ mol} \cdot \text{dm}^{-3}$) (25); see Fig. 3. From bottom to top: KBr, NaBr, KCl, and NaCl additions (calculations based on Eq. 12 and parameters from Table 2) to buffer.

Osmotic Compressibility(χ_{osm})



$$\chi_{\text{osm}} = \beta(\partial P / \partial \rho)_{N,T}$$

- 数据来源: scattering techniques (see, e.g., refs. 28 and 53).
- 实验数据来源: Rosenbaum et al. (28) determined χ_{osm} of lysozyme in acetate buffer–salt mixtures at pH 4.6.
- Fig. 7 shows our calculations of osmotic compressibilities, with $e_{\text{w}}/k_{\text{B}}$ calculated from Eq. 12 (lines), compared with the experimental data on lysozyme–NaCl mixtures (28) (symbols).

Fig. 7. Osmotic compressibility χ_{osm} for lysozyme–NaCl mixtures at pH 4.6 (symbols denote experimental data from ref. 28) and theoretical predictions (lines) for different NaCl concentrations: 0.15 (●), 0.25 (■), and 0.45 (▲) mol·dm⁻³. We changed the scale of the x axis from ρ (28) to γ concentration units.

- 文章新颖之处: Systematic experiments
- 问题: 引用参考文献的数据。
- 数据点个数。
- 启发: 力学思想融入建模之中。

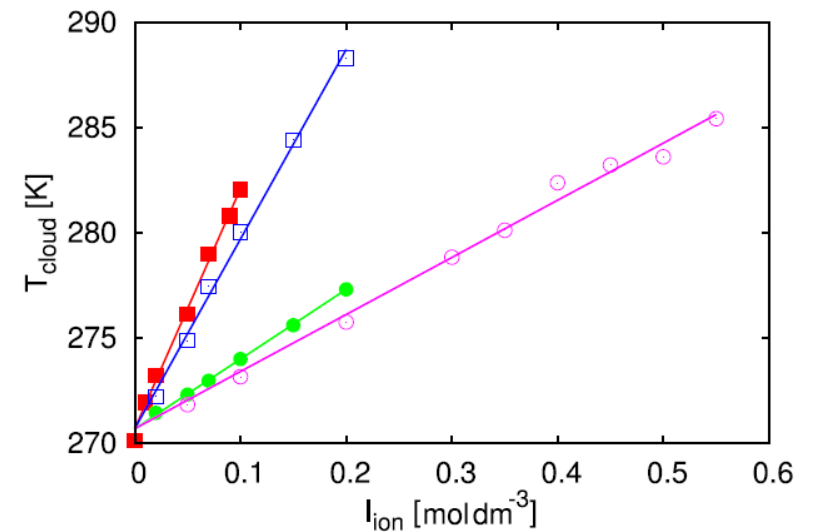


Fig. 3. T_{cloud} for lysozyme as a function of ionic strength of the added alkali-halide salts I_{ion} : symbols denote experimental data (pH 6.8, $I_{\text{tot}} = 0.6 \text{ mol} \cdot \text{dm}^{-3}$, phosphate buffer and added alkali-halide salts) (25) and the lines are results of Eq. 12. The parameters are from Table 2. From top to bottom: KBr (filled red square), NaBr (open blue square), KCl (filled green circle), and NaCl (open pink circle) salts.

谢谢